

**MODULATORY EFFECT OF THICAPA ON THE  
AMYLOID PRECURSOR PROTEIN  
PROCESSING PATHWAYS OF FAMILIAL  
ALZHEIMER'S DISEASE USING FIBROBLAST  
CELL LINES**

**DANESH A/L THANGESWARAN**

**UNIVERSITI SAINS MALAYSIA**

**2025**

**MODULATORY EFFECT OF THICAPA ON THE  
AMYLOID PRECURSOR PROTEIN PROCESSING  
PATHWAYS OF FAMILIAL ALZHEIMER'S  
DISEASE USING FIBROBLAST CELL LINES**

by

**DANESH A/L THANGESWARAN**

**Thesis submitted in fulfilment of the requirements  
for the degree of  
Master of Science**

**April 2025**

## ACKNOWLEDGEMENT

I would like to express my sincere gratitude to my main supervisor, Associate Professor Dr. Venugopal Balakrishnan, and co-supervisor, Professor Dr. Shaharum Shamsuddin, for their unwavering guidance, encouragement, and patience throughout this research project. Their invaluable insights and timely support were instrumental in overcoming challenges and achieving this milestone.

I am grateful to the Ministry of Higher Education for funding this research program through the TRGS grant scheme. Special thanks are extended to Jabatan Perkhidmatan Awam for providing me with the Program Pelajar Cemerlang 2022 scholarship that enabled me to pursue my Master's Degree at Universiti Sains Malaysia (USM).

I also acknowledge the assistance and advice of the science officers, lab technologists, technical staff, and lecturers from the Institute for Research in Molecular Medicine (INFORMM). Their support and the comfortable research environment provided by INFORMM were crucial for successfully completing this project.

Furthermore, I am thankful to my teammates, Navanithan, Caroline, Mohitha, Rehasri and Dharshini, for their invaluable encouragement and support with experiments throughout this project. Their contributions are deeply appreciated.

Finally, heartfelt thanks to my beloved family and friends for their unwavering support and encouragement throughout this journey. Their presence has been a source of strength during challenging times.

## TABLE OF CONTENTS

<b>ACKNOWLEDGEMENT .....</b>	<b>ii</b>
<b>TABLE OF CONTENTS.....</b>	<b>iii</b>
<b>LIST OF TABLES .....</b>	<b>vii</b>
<b>LIST OF FIGURES .....</b>	<b>ix</b>
<b>LIST OF SYMBOLS AND UNITS.....</b>	<b>xv</b>
<b>LIST OF ABBREVIATIONS.....</b>	<b>xvi</b>
<b>LIST OF APPENDICES.....</b>	<b>xviii</b>
<b>ABSTRAK .....</b>	<b>xix</b>
<b>ABSTRACT .....</b>	<b>xxi</b>
<b>CHAPTER 1 INTRODUCTION.....</b>	<b>1</b>
1.1 Background .....	1
1.2 Problem statement.....	4
1.3 Research questions .....	6
1.4 Hypothesis and research objectives.....	7
1.5 Research flow chart.....	8
<b>CHAPTER 2 LITERATURE REVIEW.....</b>	<b>9</b>
2.1 Alzheimer's disease (AD).....	9
2.2 Classification of AD.....	10
2.3 Symptoms.....	11
2.4 Diagnosis.....	12
2.5 Molecular pathogenesis.....	13
2.5.1 Pathological hallmarks .....	13
2.5.2 Amyloid Precursor Protein (APP).....	14
2.5.3 APP cleaving proteases .....	15
2.5.4 APP processing pathways .....	19
2.6 Amyloid-beta (A $\beta$ ).....	20
2.6.1 Amyloid cascade hypothesis .....	20
2.6.2 A $\beta$ conformations.....	21
2.6.3 A $\beta$ toxicity.....	23

2.7	Oxidative Stress (OS).....	24
2.8	Pharmacotherapy.....	25
2.9	Potential therapeutics targeting amyloidogenic processing of APP.....	28
2.10	Tetrahydroisoquinoline (THIQ) derivatives.....	29
2.10.1	Background of THIQ derivatives.....	29
2.10.2	THICAPA .....	31
2.11	Fibroblast as a potential AD research model .....	32
<b>CHAPTER 3 MATERIALS AND METHODOLOGY.....</b>		<b>34</b>
3.1	Materials and equipment .....	34
3.1.1	MEM complete media.....	39
3.1.2	Phosphate Buffered Saline (PBS) .....	39
3.1.3	Cell lysis solution.....	39
3.1.4	Preparation of THICAPA.....	39
3.1.5	Preparation of A $\beta$ 42 .....	40
3.1.6	Preparation of buffer and reagents .....	40
3.2	Cell culture .....	42
3.2.1	Cell lines.....	42
3.2.2	Cell thawing .....	42
3.2.3	Sub-culturing of cells .....	42
3.2.4	Cryopreserving cells.....	43
3.3	<i>In vitro</i> THICAPA cytotoxicity evaluation.....	43
3.4	A $\beta$ scavenging assay .....	45
3.4.1	Screening for IC <sub>50</sub> of aged A $\beta$ 42 oligomers.....	45
3.4.2	THICAPA-mediated cytoprotective assessment.....	46
3.5	qRT-PCR.....	48
3.5.1	RNA extraction .....	48
3.5.2	RNA concentration and purity evaluation.....	49
3.5.3	Agarose gel electrophoresis .....	49
3.5.4	Complementary DNA Synthesis.....	49
3.5.5	cDNA template optimisation.....	50
3.5.6	Primer assay optimisation .....	51
3.5.7	qPCR amplification efficiency .....	51

3.5.8	mRNA expression analysis .....	52
3.6	Western blot analysis .....	53
3.6.1	Cell lysate preparation.....	53
3.6.2	Estimation of protein concentration .....	54
3.6.3	SDS-PAGE procedure.....	54
3.6.4	Coomassie Brilliant Blue staining.....	55
3.6.5	Western blot .....	56
3.7	ELISA.....	58
3.7.1	Preparation of conditioned media .....	58
3.7.2	Preparation of cell lysate.....	58
3.7.3	Sandwich ELISA.....	59
3.8	Detection of ROS .....	62
	<b>CHAPTER 4 RESULTS AND DISCUSSIONS .....</b>	<b>64</b>
4.1	THICAPA as the compound of interest in this study.....	64
4.2	Skin-derived fibroblast cell lines as an AD study model .....	64
4.3	<i>In vitro</i> cytotoxicity evaluation of THICAPA on AG06840 and GM05879 cell lines .....	65
4.4	A $\beta$ scavenging assay .....	71
4.4.1	<i>In vitro</i> cytotoxicity evaluation of aged A $\beta$ 42 oligomers .....	72
4.4.2	THICAPA-mediated cytoprotective assessment.....	74
4.5	qRT-PCR.....	77
4.5.1	Quality of extracted RNA from fibroblasts.....	77
4.5.2	Template optimisation.....	79
4.5.3	Primer assay optimisation .....	80
4.5.4	PCR amplification efficiency .....	82
4.5.5	qRT-PCR amplification .....	84
4.6	Western blot .....	90
4.6.1	APP .....	90
4.6.2	ADAM10.....	94
4.6.3	BACE1 .....	97
4.6.4	PSEN1 .....	98
4.7	Sandwich ELISA.....	101
4.7.1	sAPP $\alpha$ .....	101

4.7.2	sAPP $\beta$ .....	104
4.7.3	CTF $\beta$ .....	105
4.7.4	A $\beta$ 40.....	106
4.7.5	A $\beta$ 42.....	108
4.8	ROS detection assay.....	113
4.9	General discussion.....	119
<b>CHAPTER 5 CONCLUSION AND FUTURE RECOMMENDATIONS.....</b>		<b>122</b>
5.1	Conclusion.....	122
5.2	Limitations of this study.....	124
5.3	Future recommendations .....	124
<b>REFERENCES .....</b>		<b>125</b>
<b>APPENDICES</b>		
<b>LIST OF PUBLICATIONS</b>		

## LIST OF TABLES

	<b>Page</b>
Table 2.1	List of cleavage enzymes, isoforms, functions and its relevant information.....17
Table 2.2	The list of FDA-approved drugs for AD treatment and the reported side effects (Alzheimer’s Association, 2021). .....27
Table 2.3	Type of therapeutics developed against cleavage enzymes, therapeutic focus and associated side effects to treat Alzheimer’s disease. ....28
Table 3.1	List of reagents.....34
Table 3.2	List of equipment. ....36
Table 3.3	List of cell lines. ....37
Table 3.4	List of antibodies.....37
Table 3.5	List of kits. ....38
Table 3.6	List of primers. ....38
Table 3.7	The list of stock solutions and recipes for SDS-PAGE.....41
Table 3.8	Formulation of the polyacrylamide resolving gel (8%). .....55
Table 3.9	The formulation of polyacrylamide stacking gel (4%). .....55
Table 3.10	The optimal conditions for the Western blot procedure.....57
Table 3.11	The type of samples and standards used to quantify proteins in ELISA. ....61
Table 3.12	The optimal conditions of ELISA experiments for the respective proteins.....61
Table 4.1	The IC <sub>50</sub> values of THICAPA on AG06840 and GM05879 cell lines at varying concentrations and three different time points. The data

are expressed as the mean  $\pm$  SEM of three independent experiments.

	.....	69
Table 4.2	Total RNA concentration and absorbance ratio. ....	78
Table 4.3	Cq value of the GAPDH gene in the GM05879 cell line with 1% DMSO addition with varying cDNA concentrations. ....	79
Table 4.4	Tabular result of the primer efficiency test of APP, ADAM10, BACE1, PSEN1, and GAPDH genes in the GM05879 cell line with the addition of 1% DMSO (control). ....	83
Table 4.5	The summary of experimental findings of qRT-PCR, Western blot and ELISA in this study .....	121

## LIST OF FIGURES

	<b>Page</b>
Figure 1.1	Research flowchart of the current study.....8
Figure 2.1	Schematic diagram of the APP processing pathway comprising the amyloidogenic pathway (pink background) and non-amyloidogenic pathway (green background). Adapted from Müller <i>et al.</i> (2017)..20
Figure 2.2	The structural confirmation of A $\beta$ peptides. Adapted from Chen <i>et al.</i> (2017).....22
Figure 2.3	The comprehensive pathway of THIQ derivatives in AD treatment. Adapted from Thangeswaran <i>et al.</i> (2024). ....30
Figure 2.4	The chemical structure of THICAPA (Tan et al., 2023).....31
Figure 3.1	Timeline of the WST-1 assay on AG06840 and GM05879 cell lines. Cells were first seeded with complete media and incubated for 24 hours. Then, the existing media was replaced with THICAPA-treated media at three different time points of 24, 48, and 72 hours .....44
Figure 3.2	Timeline of the A $\beta$ 42 scavenging assay evaluated using WST-1. Cells were first seeded with complete media. After 24 hours, 5 $\mu$ M aged A $\beta$ 42 oligomers and THICAPA of varying concentrations were introduced to the GM05879 fibroblasts. WST-1 assay was carried out after 72 hours of treatment. ....47
Figure 4.1	Cell viability percentage of AG06840 cell line treated with serially diluted THICAPA with concentration range of 1.95–500 $\mu$ M at three different time points (n= 3). ....67
Figure 4.2	Cell viability percentage of GM05879 cell line treated with serially diluted THICAPA with concentration range of 1.95–500 $\mu$ M at three different time points (n= 3). ....69

Figure 4.3	Cell viability percentage of the GM05879 cell line treated with 10 different concentrations of aged A $\beta$ 42 oligomers ranging from 0.2–50 $\mu$ M for 72 hours (n= 3). The IC <sub>50</sub> of aged A $\beta$ 42 oligomers was 4.95 $\mu$ M, as indicated on the graph. ....73
Figure 4.4	Cell viability percentage of GM05879 fibroblasts treated with 5 $\mu$ M aged A $\beta$ 42 oligomers and 12 different concentrations of THICAPA ranging from 5–60 $\mu$ M for 72 hours. The data are presented as the mean $\pm$ SEM of three independent experiments; *** <i>p</i> < 0.001; ns indicates an insignificant difference vs cell co-incubated with aged A $\beta$ 42 oligomers; one-way ANOVA, followed by Dunnett’s <i>post hoc</i> analysis.....75
Figure 4.5	The quality of RNA was verified using 1% (w/v) agarose gel visualised under UV light, and the image was captured using the InGenius Bioimaging System. Lane M depicts the RNA marker, A refers to GM05879 fibroblasts with 1% DMSO addition, B represents AG06840 fibroblasts with 1% DMSO addition, and C indicates 50 $\mu$ M THICAPA-treated AG06840 fibroblasts.....78
Figure 4.6	Standard curve of the GAPDH gene at varying concentrations in GM05879 cell line with 1% DMSO addition (n= 3).....80
Figure 4.7	Standard curve of the APP primer at different concentrations of (A) 20 $\times$ , (B) 10 $\times$ , (C) 5 $\times$ , (D) 2.5 $\times$ , and (E) 1.25 $\times$ on GM05879 cell line with 1% DMSO addition (n= 3).....81
Figure 4.8	The relative mRNA expression of APP in AG06840 fibroblasts with 1% DMSO addition (untreated) and 50 $\mu$ M THICAPA-treated AG06840 fibroblasts (treated) normalised to GM05879 fibroblasts with 1% DMSO addition (control). The data are presented as the mean $\pm$ SEM of the three independent experiments; *** <i>p</i> < 0.001 vs untreated fibroblasts; Student’s <i>t</i> -test.....85
Figure 4.9	The relative mRNA expression of ADAM10 in AG06840 fibroblasts with 1% DMSO addition (untreated) and 50 $\mu$ M THICAPA-treated

	AG06840 fibroblasts (treated) normalised to GM05879 fibroblasts with 1% DMSO addition (control). The data are presented as the mean $\pm$ SEM of the three independent experiments; ** $p < 0.01$ vs untreated fibroblasts; Student's <i>t</i> -test.....86
Figure 4.10	The relative mRNA expression of BACE1 in AG06840 fibroblasts with 1% DMSO addition (untreated) and 50 $\mu$ M THICAPA-treated AG06840 fibroblasts (treated) normalised to GM05879 fibroblasts with 1% DMSO addition (control). The data are presented as the mean $\pm$ SEM of the three independent experiments; ** $p < 0.01$ vs untreated fibroblasts; Student's <i>t</i> -test.....87
Figure 4.11	The relative mRNA expression of PSEN1 in AG06840 fibroblasts with 1% DMSO addition (untreated) and 50 $\mu$ M THICAPA-treated AG06840 fibroblasts (treated) normalised to GM05879 fibroblasts with 1% DMSO addition (control). The data are presented as the mean $\pm$ SEM of the three independent experiments; * $p < 0.05$ vs untreated fibroblasts; Student's <i>t</i> -test.....88
Figure 4.12	(A) The detection of two APP isoforms from the cell lysates comprising the mAPP at ~120 kDa and imAPP at ~90 kDa. (B) The densitometry analysis of the mAPP/imAPP expression observed in GM05879 fibroblasts with 1% DMSO addition (control), AG06840 fibroblasts with 1% DMSO addition (untreated), and 50 $\mu$ M THICAPA-treated AG06840 fibroblasts (treated). The relative expression normalised to the GAPDH density is expressed as the mean $\pm$ SEM from the three independent experiments; * $p < 0.05$ ; ns indicates an insignificant difference; one-way ANOVA, followed by Tukey's <i>post hoc</i> analysis. ....91
Figure 4.13	(A) The detection of an active ADAM10 isoform in the cell lysates at ~60 kDa. (B) The densitometry analysis of the ADAM10 expression observed in GM05879 fibroblasts with 1% DMSO addition (control), AG06840 fibroblasts with 1% DMSO addition

	(untreated), and 50 $\mu$ M THICAPA-treated AG06840 fibroblasts (treated). The relative expression normalised to the GAPDH density is expressed as the mean $\pm$ SEM from the three independent experiments; * $p$ < 0.05 and *** $p$ < 0.001; one-way ANOVA, followed by Tukey's <i>post hoc</i> analysis. ....95
Figure 4.14	(A) The detection of BACE1 protein expression in the cell lysates at $\sim$ 70 kDa. (B) Densitometry analysis of the BACE1 expression observed in GM05879 fibroblasts with 1% DMSO addition (control), AG06840 fibroblasts with 1% DMSO addition (untreated), and 50 $\mu$ M THICAPA-treated AG06840 fibroblasts (treated). The relative expression normalised to the GAPDH density is expressed as the mean $\pm$ SEM from the three independent experiments; * $p$ < 0.05 and ** $p$ < 0.01; ns indicates an insignificant difference; one-way ANOVA, followed by Tukey's <i>post hoc</i> analysis.....98
Figure 4.15	(A) The detection of PSEN1 protein expression in the cell lysates at $\sim$ 53 kDa. (B) Densitometry analysis of PSEN1 expression observed in GM05879 fibroblasts with 1% DMSO addition (control), AG06840 fibroblasts with 1% DMSO addition (untreated), and 50 $\mu$ M THICAPA-treated AG06840 fibroblasts (treated). The relative expression normalised to the GAPDH density is expressed as the mean $\pm$ SEM from the three independent experiments; * $p$ < 0.05; one-way ANOVA, followed by Tukey's <i>post hoc</i> analysis.....99
Figure 4.16	The sandwich ELISA of sAPP $\alpha$ in GM05879 fibroblasts with 1% DMSO addition (control), AG06840 fibroblasts with 1% DMSO addition (untreated), and 50 $\mu$ M THICAPA-treated AG06840 fibroblasts (treated) quantified from the conditioned media. The data are presented as the mean $\pm$ SEM of the three independent experiments; * $p$ < 0.05 and *** $p$ < 0.001; one-way ANOVA, followed by Tukey's <i>post hoc</i> analysis. ....102

Figure 4.17	The sandwich ELISA of sAPP $\beta$ in GM05879 fibroblasts with 1% DMSO addition (control), AG06840 fibroblasts with 1% DMSO addition (untreated), and 50 $\mu$ M THICAPA-treated AG06840 fibroblasts (treated) quantified from the conditioned media. The data are presented as the mean $\pm$ SEM of the three independent experiments; * $p$ < 0.05 and *** $p$ < 0.001; one-way ANOVA, followed by Tukey's <i>post hoc</i> analysis. ....104
Figure 4.18	The sandwich ELISA of CTF $\beta$ in GM05879 fibroblasts with 1% DMSO addition (control), AG06840 fibroblasts with 1% DMSO addition (untreated), and 50 $\mu$ M THICAPA-treated AG06840 fibroblasts (treated) quantified from the cell lysates. The data are presented as the mean $\pm$ SEM of the three independent experiments; *** $p$ < 0.001; one-way ANOVA, followed by Tukey's <i>post hoc</i> analysis. ....106
Figure 4.19	The sandwich ELISA of A $\beta$ 40 in GM05879 fibroblasts with 1% DMSO addition (control), AG06840 fibroblasts with 1% DMSO addition (untreated), and 50 $\mu$ M THICAPA-treated AG06840 fibroblasts (treated) quantified from the conditioned media. The data are presented as the mean $\pm$ SEM of the three independent experiments; ** $p$ < 0.01 and *** $p$ < 0.001; one-way ANOVA, followed by Tukey's <i>post hoc</i> analysis. ....107
Figure 4.20	The sandwich ELISA of A $\beta$ 40 in GM05879 fibroblasts with 1% DMSO addition (control), AG06840 fibroblasts with 1% DMSO addition (untreated), and 50 $\mu$ M THICAPA-treated AG06840 fibroblasts (treated) quantified from the cell lysates. The data are presented as the mean $\pm$ SEM of the three independent experiments; *** $p$ < 0.001; one-way ANOVA, followed by Tukey's <i>post hoc</i> analysis. ....108
Figure 4.21	The sandwich ELISA of A $\beta$ 42 in GM05879 fibroblasts with 1% DMSO addition (control), AG06840 fibroblasts with 1% DMSO

	addition (untreated), and 50 $\mu$ M THICAPA-treated AG06840 fibroblasts (treated) quantified from the conditioned media. The data are presented as the mean $\pm$ SEM of the three independent experiments; *** $p$ < 0.001; one-way ANOVA, followed by Tukey's <i>post hoc</i> analysis. ....109
Figure 4.22	The sandwich ELISA of A $\beta$ 42 in GM05879 fibroblasts with 1% DMSO addition (control), AG06840 fibroblasts with 1% DMSO addition (untreated), and 50 $\mu$ M THICAPA-treated AG06840 fibroblasts (treated) quantified from the cell lysates. The data are presented as the mean $\pm$ SEM of the three independent experiments; *** $p$ < 0.001; one-way ANOVA, followed by Tukey's <i>post hoc</i> analysis.....110
Figure 4.23	The relative ROS level in GM05879 fibroblasts with 1% DMSO addition (control), AG06840 fibroblasts with 1% DMSO addition (untreated), and 50 $\mu$ M THICAPA-treated AG06840 fibroblasts (treated). The RFU measurement was normalised against the RFU of the control fibroblasts. The data are presented as the mean $\pm$ SEM of the three independent experiments; * $p$ < 0.05 and ** $p$ < 0.01; one-way ANOVA, followed by Tukey's <i>post hoc</i> analysis .....114
Figure 4.24	The intracellular fluorescence emission in (A) GM05879 fibroblasts with 1% DMSO addition (control), (B) AG06840 fibroblasts with 1% DMSO addition (untreated), and (C) 50 $\mu$ M THICAPA-treated AG06840 fibroblasts (treated); white arrows indicate the intracellular fluorescent emission due to oxidation by ROS. Image captured under 20 $\times$ magnification. ....116
Figure 5.1	The possible modulatory action of THICAPA on the APP processing pathway in AG06840 fibroblasts. The light green background (left) represents the non-amyloidogenic pathway, while the pink background (right) denotes the amyloidogenic pathway. ....123

## LIST OF SYMBOLS AND UNITS

%	Percentage
±	Plus/minus
~	Approximately
°C	Degree Celsius
>	More than
<	Less than
α	Alpha
β	Beta
γ	Gamma
Δ	Delta
R <sup>2</sup>	R-squared
× g	Gravitational force
IC <sub>50</sub>	Half-maximal inhibitory concentration
kDa	Kilodalton
kb	Kilobase
L	Litre
mM	Millimolar
mL	Millilitre
ng	Nanogram
nm	Nanometre
μM	Micromolar
pg	Picogram
RFU	Relative fluorescence unit
μL	Microlitre
μg	Microgram
v/v	Volume per volume
w/v	Weight per volume

## LIST OF ABBREVIATIONS

AD	Alzheimer's disease
ADAM10	A Disintegrin and Metalloproteinase domain-containing protein 10
APP	Amyloid precursor protein
A $\beta$	Amyloid beta
BACE1	Beta-site amyloid precursor protein cleaving enzyme 1
BBB	Blood-brain barrier
cDNA	Complementary DNA
CNS	Central nervous system
Cq	Quantification cycle
CT	Cycle threshold
CSF	Cerebrospinal fluid
CTF $\beta$	C-terminal fragment beta
ELISA	Enzyme-linked immunosorbent assay
ER	Endoplasmic reticulum
fAD	Familial Alzheimer's disease
FBS	Fetal bovine serum
FDA	Food and Drug Administration
GAPDH	Glyceraldehyde-3-phosphate dehydrogenase
IUPAC	International Union of Pure and Applied Chemistry
MCI	Mild cognitive impairment
MEM	Minimum Essential Medium Eagle
MRI	Magnetic resonance imaging
NEAA	Non-essential amino acid
NFT	Neurofibrillary tangles
NSAID	Non-steroidal anti-inflammatory drug
NTC	No template control
OD	Optical density
PBS	Phosphate-buffered saline
PET	Positron emission tomography

PSEN	Presenilin
qRT-PCR	Real-Time Quantitative Reverse Transcription - Polymerase Chain Reaction
RNA	Ribonucleic acid
ROS	Reactive oxidative stress
ROX	6-carboxyl-X-rhodamine
sAPP $\alpha$	Soluble amyloid precursor protein alpha
sAPP $\beta$	Soluble amyloid precursor protein beta
SEM	Standard error mean
TBE	Tris/Borate/EDTA buffer
TBS	Tris-buffered saline
THICAPA	3-[[[(3S)-1,2,3,4-Tetrahydroisoquinoline-3 carbonyl]amino] propanoic acid
THIQ	Tetrahydroisoquinoline
UV	Ultraviolet
WHO	World Health Organization

## LIST OF APPENDICES

Appendix A	Certificate of analysis of THICAPA
Appendix B	In vitro cytotoxicity
Appendix C	A $\beta$ 42 scavenging assay
Appendix D	qRT-PCR
Appendix E	Western blot
Appendix F	ELISA
Appendix G	ROS detection assay

**KESAN MODULASI THICAPA TERHADAP TAPAKJALAN PROSES  
PROTEIN PREKURSOR AMILOID PENYAKIT ALZHEIMER *FAMILIAL*  
MENGUNAKAN TITISAN SEL FIBROBLAS**

**ABSTRAK**

Penyakit Alzheimer *familial* (fAD) adalah gangguan neurologi yang diwarisi dan tidak dapat dipulihkan yang dicirikan oleh pengumpulan amiloid-beta ( $A\beta$ ) toksik. Kehadiran simptom fAD adalah membimbangkan, kerana belum ada ubat tersedia untuk menyembuhkan penyakit ini. THICAPA adalah sebatian baru yang tergolong dalam kumpulan kimia jenis amina, iaitu tetrahydroisoquinoline (THIQ). Kajian THICAPA sebelumnya telah melaporkan kesan neuroprotektif dalam model transgenik *Drosophila melanogaster* (*D. melanogaster*). Kajian ini, menyiasat kesan modulasi THICAPA ke atas tapakjalan proses protein prekursor amiloid (APP) dengan menggunakan titisan sel fibroblas yang berasal dari kulit pesakit fAD (AG06840). Kajian ini menggunakan asai WST-1 untuk menilai sitotoksiti dan pengebasan THICAPA, serta teknik qRT-PCR dan Western blot untuk menganalisis ekspresi gen dan protein, masing-masing. Selain itu, kuantifikasi protein dikaji menggunakan ELISA, dan tahap spesies oksigen reaktif (ROS) telah diukur menggunakan asai DCFDA. Asai sitotoksik THICAPA mendedahkan kesan ketoksikan yang tidak ketara terhadap AG06840 dan titisan sel fibroblas berasal dari kulit yang sihat (GM05879) pada tiga titik masa berbeza, 24, 48 dan 72 jam. Ujian pengebasan  $A\beta$  menunjukkan THICAPA mempunyai kesan penghapusan oligomer  $A\beta_{42}$  berumur yang tinggi pada 50  $\mu$ M dalam titisan sel fibroblas GM05879. Seterusnya, THICAPA telah mengurangkan ekspresi gen APP dan nisbah ekspresi protein APP matang dan tidak matang (mAPP/imAPP). Kedua-dua gen dan ekspresi protein BACE1 dan PSEN1 dalam

tapakjalan amyloidogenik telah berkurangan, masing-masing menandakan pengurangan aktiviti enzim  $\beta$ - dan  $\gamma$ -secretase. Sebaliknya, ekspresi gen dan protein ADAM10 yang tinggi menandakan peningkatan aktiviti enzim  $\alpha$ -secretase dalam tapakjalan bukan amyloidogenik. Kuantifikasi protein yang dihasilkan daripada tapakjalan proses APP telah menunjukkan pengurangan ketara sAPP $\beta$ , CTF $\beta$ , A $\beta$ 40, dan A $\beta$ 42 daripada tapakjalan amyloidogenik, dan peningkatan sAPP $\alpha$  daripada tapakjalan bukan amyloidogenik. Pengesanan ROS secara *in vitro* telah mendedahkan bahawa rawatan THICAPA mengurangkan pengeluaran ROS dalam titisan sel AG06840, berpotensi oleh amyloidogenesis yang dikurangkan. Ringkasnya, kajian ini menunjukkan THICAPA mempunyai potensi terapeutik untuk terus diformulasi sebagai terapi sasaran efektif untuk fAD dengan meningkatkan tapakjalan bukan amyloidogenik dan mengurangkan tapakjalan amyloidogenic.

**MODULATORY EFFECT OF THICAPA ON THE AMYLOID PRECURSOR  
PROTEIN PROCESSING PATHWAYS OF FAMILIAL ALZHEIMER'S  
DISEASE USING FIBROBLAST CELL LINES**

**ABSTRACT**

Familial Alzheimer's disease (fAD) is a hereditary and irreversible neurological disorder characterised by the accumulation of toxic amyloid-beta ( $A\beta$ ). The prevalence of fAD symptoms is concerning as there are no available therapeutic solutions to cure this disease. THICAPA is a novel compound belonging to the tetrahydroisoquinoline (THIQ) group of amines, which reported the neuroprotective effects on the AD transgenic *Drosophila melanogaster* (*D. melanogaster*) model. Therefore, this study investigated the modulatory effect of THICAPA on the Amyloid Precursor Protein (APP) processing pathway using the fAD patient skin-derived fibroblast cell line (AG06840). This study utilized WST-1 assay to assess cytotoxicity and scavenging potency of THICAPA, while qRT-PCR and Western blot to analyse gene and protein expressions, respectively. Additionally, protein quantification was performed using ELISA and intracellular reactive oxygen species (ROS) levels were measured using the DCFDA assay. The cytotoxicity assay recorded the insignificant toxic effect of THICAPA towards AG06840 and healthy skin-derived fibroblast cell line (GM05879) at three different time points of 24, 48, and 72 hours. The subsequent  $A\beta$  scavenging assay showed that 50  $\mu$ M THICAPA exerted a potent scavenging effect on aged  $A\beta_{42}$  oligomers in the GM05879 fibroblasts cell line. THICAPA reduced the APP gene expression and the mature/immature APP protein (mAPP/imAPP) expression ratio. Both gene and protein expressions of BACE1 and PSEN1 in the amyloidogenic pathway were also diminished, indicating the

downregulation of the  $\beta$ - and  $\gamma$ -secretase activities, respectively. In contrast, the increased ADAM10 gene and protein expressions signify the upregulation of the  $\alpha$ -secretase activity in the non-amyloidogenic pathway. In this regard, the quantification of proteins produced from the APP processing pathway displayed a significant reduction of sAPP $\beta$ , CTF $\beta$ , A $\beta$ 40, and A $\beta$ 42 from the amyloidogenic pathway and elevated sAPP $\alpha$  from the non-amyloidogenic pathway. The *in vitro* ROS detection revealed that THICAPA treatment mitigated the intracellular ROS production in AG06840 fibroblasts, potentially via downregulation of amyloidogenesis. In summary, this study revealed the therapeutic potential of THICAPA by upregulating the non-amyloidogenic pathway while suppressing amyloidogenic pathway and amyloidogenesis, attesting its effectiveness as a targeted therapy for fAD.

## CHAPTER 1

### INTRODUCTION

#### 1.1 Background

Alzheimer's disease (AD) is an irreversible neurological disorder that primarily affects neurons and the brain. This disease develops slowly over time, marked by pathophysiological brain changes that occur before the onset of noticeable clinical manifestations. As such, AD is the most prevalent form of dementia detected in elderly individuals, contributing up to 80% of all dementia cases worldwide (Alzheimer's Association, 2021). This disease poses a significant healthcare and socio-economic burden, requiring over USD 179 billion for the clinical management of AD patients (Monfared *et al.*, 2022). According to the World Health Organisation (WHO) report in 2021, AD affects over 55 million people globally, with roughly 10 million new cases being diagnosed each year (WHO, 2021). It is estimated that the annual economic burden associated with the clinical management of AD patients will reach a staggering USD 2.62 trillion, with further projections indicating a ten-fold surge from 2021 to 2041 (Jun *et al.*, 2024). The deaths attributable to AD have also doubled, signifying a continuous upward trajectory, partially driven by the steady population growth and demographic shifts toward an ageing population.

Malaysia is experiencing an accelerated transition towards an ageing society driven by rapid demographic shifts. In view of this, there is a growing focus on AD in Malaysia, with projections suggesting that it will further worsen in the near future, highlighting the need for more comprehensive research and effective interventions. In Malaysia, approximately 260, 000 individuals, constituting roughly 8.5% of the elderly

population with dementia, require 24-hour care in the late stages of the disease (Alzheimer's disease Foundation Malaysia, 2020; WHO, 2021). Given that the elderly population in Malaysia is projected to triple by 2050, this increase is expected to lead to a 312% surge in the number of AD cases (Benoist *et al.*, 2022; Ong *et al.*, 2024).

Hypothetically, the neurodegenerative cascade in AD is associated with uncontrolled microglial activation, manifested by the build-up of amyloid- $\beta$  (A $\beta$ ) plaques and Neurofibrillary Tangles (NFTs) due to hyperphosphorylated tau (Kamble *et al.*, 2024). Among them, the accumulation of A $\beta$  plaques plays the dominant role in inducing tau pathology. This neuroinflammatory response involves the secretion of neurotoxins and inflammatory factors, which are believed to contribute to progressive neuronal loss, ultimately resulting in memory decline and cognitive dysfunction. This effect highlights the substantial and rapidly escalating healthcare challenges posed by AD patients.

There are two main categories of AD: familial AD (fAD) and sporadic AD (sAD). The A $\beta$  peptides in fADs originate from a transmembrane protein called Amyloid Precursor Protein (APP) through  $\beta$ - and  $\gamma$ -secretase cleavage, demonstrating a robust genetic association (Cho *et al.*, 2022). Notably, a reduction in  $\alpha$ -secretase activity promotes the formation of A $\beta$  peptides, which potentially contributes to the accumulation of A $\beta$  plaques, neuroinflammation, neuronal damage, and, ultimately, dementia (Kamble *et al.*, 2024). Genetic mutations in active gene coding of APP, Presenilin 1 (PSEN1), and Presenilin 2 (PSEN2) appear to increase the risk of fAD, thus strengthening their direct involvement in AD pathogenesis.

The fAD poses a greater threat to the healthcare system due to its inheritance, early onset and its potential to affect individuals as young as 20 years old. Moreover, fAD is

mostly detected when the patient has aged and the symptoms have worsened (WHO, 2021). Studies have reported that an upregulated amyloidogenic pathway produces A $\beta$  isoforms, such as A $\beta$ 40 and A $\beta$ 42, which are highly toxic and tend to aggregate in neurons to form A $\beta$  plaques (Ayton & Bush, 2021). Despite the fact that the A $\beta$  pathology was identified in AD patients approximately 20 years before the clinical onset, there are yet any established drugs to cure or reverse the disease (Jia *et al.*, 2023). Concurrently, most of the drugs tested in clinical trials have failed to block the disease progression, underscoring the significant need to formulate effective treatments to reverse AD progression (Ord *et al.*, 2013).

In recent decades, research on 1,2,3,4-tetrahydroisoquinoline (THIQ) moieties has yielded several promising therapeutic candidates to treat diverse conditions, including neurological disorders, gout, pain, and cancer (Pyne & Martin, 2022). This unique heterocyclic scaffold belongs to the secondary amine class and is endogenously produced in the brain during the degradation of dopamine, which can readily cross the Blood-brain Barrier (BBB) (Hényková *et al.*, 2022). Studies on THIQ derivatives have demonstrated their ability to suppress A $\beta$  production directly (Fang *et al.*, 2019), provide synaptoprotection against A $\beta$ -induced toxicity (Wang *et al.*, 2020), and offer neuroprotective potential through the inhibition of Reactive Oxygen Species (ROS) production (Ting *et al.*, 2021). THIQ derivatives have also shown promising results in modulating APP proteolytic cleavage (Zhang *et al.*, 2011).

A recent study by Tan *et al.* (2023) highlighted the neuroprotective effect of a novel THIQ derivative known as THICAPA, with an IUPAC name of 3-[[[(3S)-1,2,3,4-tetrahydroisoquinoline-3 carbonyl]amino] propanoic acid. The study revealed that

THICAPA alleviates AD-related defects in rat pheochromocytoma nerve cells (PC12) and transgenic *Drosophila melanogaster* (*D. melanogaster*) expressing human A $\beta$ 42. Although THICAPA treatment significantly boosted cell survival and enhanced cell growth when incubated with toxic A $\beta$ 42 peptides, the molecular interaction of THICAPA and its impact on human-derived cell lines has not been investigated. Given the significant reduction of A $\beta$ 42 aggregation by THICAPA in AD transgenic *D. melanogaster*, it is essential to explore the modulatory effect of THICAPA in the APP processing pathway, which mainly produces toxic A $\beta$  peptides.

## **1.2 Problem statement**

The surge in AD cases is alarming since 99.6% of AD drug testing in clinical trials has recorded the highest failure rates compared to all other diseases globally (Jabir *et al.*, 2021). There are also no effective treatments capable of curing or reversing AD progression. The available therapies only address the disease's symptoms, offering limited prevention or slowing down its progression (Kamble *et al.*, 2024). Hence, the inherent complexity and association with specific gene mutations of fAD present a significant burden to the healthcare system and economy.

Therapeutic strategies have focused on the neurotoxicity of A $\beta$  accumulation as the primary target to alleviate AD pathogenesis. Notably, the APP processing pathway plays a crucial role in the production of A $\beta$  peptides, where imbalances in the production and clearance lead to its accumulation (Delaby *et al.*, 2022). Nevertheless, therapeutic efforts on addressing the endpoint (A $\beta$  inhibition) have failed to offer substantial success in AD treatments, warranting further assessment of the APP processing pathway. In light

of the absence of current therapies that can cure or reverse AD progression, the discovery of novel AD treatment drugs is paramount.

THICAPA has recently emerged as a promising AD therapeutic candidate in pre-clinical studies, evident by its ability to inhibit A $\beta$ 42 aggregation and extend the lifespan of transgenic AD *D. melanogaster* (Tan *et al.*, 2023). Despite its promising outcome, the modulatory effect of THICAPA on the APP processing pathway is still limited. Thus, a critical knowledge gap regarding its modulatory effect on AD pathogenesis exists, especially in human-derived cell lines, and needs to be explored. In particular, the key challenge in developing effective AD therapies is the lack of understanding of the influence of genes and proteins on A $\beta$  production via the APP processing pathway, as well as the extent of THICAPA's modulatory effect on this pathway and its impact on disease progression. Thus, there is a need to investigate the modulatory effect of THICAPA in the APP processing pathway using the fAD patient-derived cell line to shed light on advancing targeted therapies and optimising drug formulations for AD treatments.

### **1.3 Research questions**

Based on the arguments listed in the introduction and problem statement sections concerning the role of THICAPA in fAD pathogenesis, several research questions (RQs) were established as follows:

**RQ1:** Does THICAPA exhibit any toxicity and possess scavenging properties against aged A $\beta$ 42 oligomers-induced cytotoxicity to fibroblast cell lines?

**RQ2:** How does THICAPA impact the gene and protein expression levels involved in the APP processing pathway?

**RQ3:** How does THICAPA influence the proteins produced from the APP processing pathway?

**RQ4:** Does THICAPA exhibit any protective effect against ROS production by reducing amyloidogenesis?

#### **1.4 Hypothesis and research objectives**

This study hypothesises that THICAPA modulates APP processing by promoting the non-amyloidogenic pathway while suppressing the amyloidogenic pathway, thereby reducing intracellular ROS production in fAD pathogenesis. This study aims to elucidate the effect of THICAPA modulation in the APP processing pathway using the fAD patient skin-derived fibroblast cell line. The aim of this study is achieved by formulating the following specific objectives:

1. To assess the cytotoxicity of THICAPA in AG06840 and GM05879 cell lines and its scavenging effect against toxic A $\beta$ 42 oligomers in the GM05879 cell line using WST-1 assay.
2. To evaluate the effect of THICAPA on the genes and protein expression levels of APP, ADAM10, BACE1, and PSEN1 in the APP processing pathway using qRT-PCR and Western blot, respectively.
3. To quantify the sAPP $\alpha$ , sAPP $\beta$ , CTF $\beta$ , A $\beta$ 40, and A $\beta$ 42 proteins produced via the APP processing pathway using the sandwich ELISA method.
4. To validate the protective potential of THICAPA by evaluating ROS production associated with amyloidogenesis.

## 1.5 Research flow chart

Figure 1.1 outlines the research flowchart of this study.

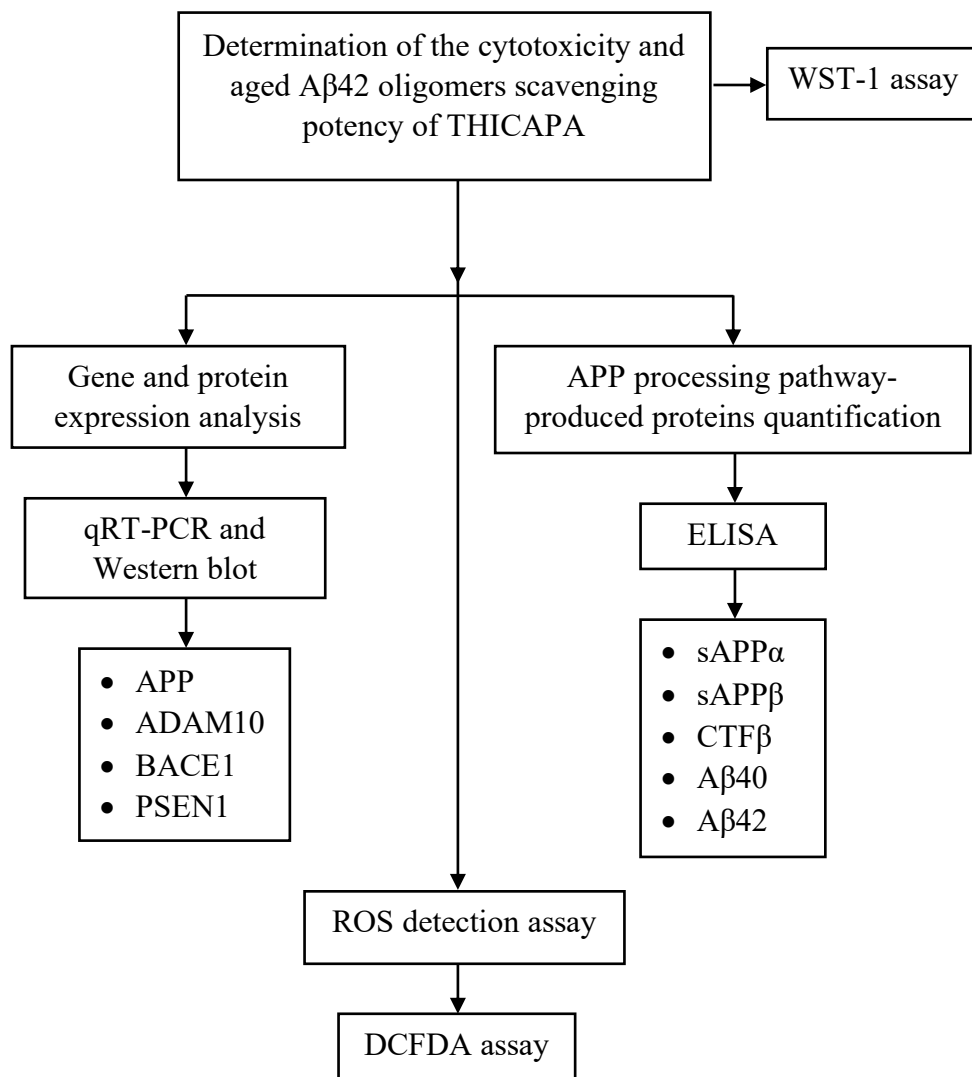


Figure 1.1 Research flowchart of the current study.

## CHAPTER 2

### LITERATURE REVIEW

#### 2.1 Alzheimer's disease (AD)

The umbrella term “neurodegenerative disease” encompasses an extensive range of chronic or progressive brain disorders known as dementia. This disease primarily affects the neurons, especially with higher prevalence in the ageing population (WHO, 2021). Hence, the global shift towards an increasingly ageing population has attracted significant attention worldwide, given its association with this particular health disorder. In particular, AD is the most prevalent form of dementia and accounts for nearly 80% of all reported dementia cases in the ageing population (Hou *et al.*, 2019). This disease disproportionately affects the elderly population, with an estimated prevalence exceeding 90% among individuals aged 65 and above (Lindemer *et al.*, 2017; Tarantini *et al.*, 2017). Moreover, recent reports have shown a rise in AD cases among young people as early as 20 years old due to the presence of genetic mutation, which accounts for less than 2% of all diagnosed AD cases (Jia *et al.*, 2023).

AD is also the fifth leading cause of death in the elderly population, comprising 4.4% of mortalities worldwide (Nichols *et al.*, 2019). The escalating trend in AD cases signifies a time-dependent exponential increase in AD patients, which doubles every five years (Moreno *et al.*, 2022). Geographically, it has become an alarming social and public health issue in developed countries (Trevisan *et al.*, 2019), with a higher reported prevalence among Europeans than Asians (World Alzheimer Report, 2021). In terms of gender, women are more susceptible to AD than men due to their longer life expectancy (Niu *et al.*, 2017).

In 2022 alone, the global prevalence of dementia was estimated at around 55 million people (Alzheimer's disease International, 2022; Ong *et al.*, 2024). In addition, approximately USD 179 billion is spent annually on the clinical management of AD patients worldwide. In Malaysia, the prevalence of AD was approximated at 260, 000 people, while it stands at 108<sup>th</sup> position in the world ranking for the total number of AD cases diagnosed. It requires roughly MYR 1.2 million in allocations annually for the clinical management of AD patients (Ong *et al.*, 2024). This condition contributes significantly to the country's healthcare and economic burden. Statistically, the National Health and Morbidity Survey reported that 8.5% of Malaysians over 60 years old are affected by dementia (Ganapathy *et al.*, 2020). As Malaysia is expected to become an ageing nation by 2030, with 15% of its population being classified as senior citizens, the situation could be alarming. AD cases are projected to increase drastically, with the disease expected to develop every 33 seconds and reach 150 million cases by 2050 (National Institute of Aging, 2021).

## **2.2 Classification of AD**

The International Statistical Classification of Diseases and Health-related Problems, 11<sup>th</sup> revision (ICD-11) (Harrison *et al.*, 2021) and the Diagnostic and Statistical Manual of Mental Disorders, 5<sup>th</sup> edition, text revision (DSM-5-TR) (American Psychiatric Association, 2021) have classified AD into two subtypes: familial AD (fAD) and sporadic AD (sAD). Over 90% of AD cases are classified as sAD, which is known as the late onset of the disease. In contrast, fAD is characterised by an early onset and comprises less than 10% of all AD cases. The fAD is a rare and inherited disease resulting mainly from genetic mutations of the APP, PSEN1, and PSEN2 (Deture & Dickson, 2019). The PSEN1 gene

exhibits the highest burden of reported mutations, exceedingly more than 360, followed by APP and PSEN2. It is commonly detected in individuals around the age of 35. However, a 19-year-old adolescent was reported as the youngest fAD patient in 2023, highlighting the severity of fAD, which can affect both elderly citizens as well as younger adults (Jia *et al.*, 2023). Conversely, the sAD is more common in individuals over 65 years old, manifested by complex risk factors that may overlap with fAD and are usually not caused by mutations. This underscores the heterogeneous nature and severity of fAD manifested across a wide range of age spectrum.

### **2.3 Symptoms**

Among the earliest signs of AD is neuropsychiatric symptoms, which are often underdiagnosed. The symptoms can affect more than 97% of dementia patients and tend to progress over time (Heilman & Nadeau, 2022). The early onset of neuropsychiatric symptoms in AD patients varies widely, from anxiety and hallucinations to aggression, depression, and sleep disorders. Some patients show signs of impaired cognitive systems, such as poor motor disturbance, irritability, aberrant vocalisation, and delusions.

A recent Mild Cognitive Impairment (MCI) study reported that 59% of AD patients exhibited poorer psychosocial and cognitive function (López & Altuna, 2023). This condition prevents patients from living a normal life, such as remembering memories, performing problem-solving tasks, planning their daily activities, and communicating. Moreover, 67% of AD patients with psychotic symptoms reported an accelerated cognitive decline and an increase in mortality (Arendt *et al.*, 2015). Both hallucinations and delusions are also correlated in AD patients, where delusions are more often than hallucinations (Khanna *et al.*, 2022).

## 2.4 Diagnosis

The Alzheimer's Association and dementia experts of the International Working Group have employed unique biomarkers as an essential tool for the clinical diagnosis of AD patients (Alzheimer's Association, 2021; Dulewicz *et al.*, 2022). Various neuroimaging techniques, such as Positron Emission Tomography (PET) and Magnetic Resonance Imaging (MRI), are currently used to diagnose the abnormalities and *in vivo* AD biomarkers found in patients' brain sections (Deture & Dickson, 2019). In addition, PET tracers are implemented to detect the accumulation of fibrillar A $\beta$  and cerebral tau proteins. Besides, these neuroimaging techniques are vital in diagnosing downstream AD biomarkers in both early and late-onset AD progression (Dulewicz *et al.*, 2022).

Furthermore, the Cerebrospinal Fluid (CSF) is used to detect key AD biomarkers in CSF include A $\beta$ 42 reflecting A $\beta$  deposition, hyperphosphorylated tau reflecting NFT formation, and neurofilament as a neurodegenerative marker (Leuzy *et al.*, 2022). The use of Enzyme-linked Immunosorbent Assays (ELISAs) targeting A $\beta$ 42 has consistently revealed significant reductions in CSF A $\beta$ 42 levels in AD patients (Blennow *et al.*, 2015; Zetterberg, 2019). This decrease is inversely correlated with an increase in cortical plaque burden, as confirmed by post-mortem studies and supported by *in vivo* biopsy data.

Alternatively, blood-based biomarkers offer a promising solution to the inherent drawbacks associated with CSF sampling, with researchers uncovering increasingly reproducible changes in these biomarkers related to AD diagnosis. The quantification of the plasma A $\beta$ 42/40 ratio and concentration of A $\beta$  isoforms have also emerged as a promising tool for identifying individuals with abnormal amyloid burden, as detected by CSF or PET, across the wide-range AD spectrum (West *et al.*, 2021).

## 2.5 Molecular pathogenesis

### 2.5.1 Pathological hallmarks

The most prominent pathological hallmark of AD is the aggregation of extracellular A $\beta$  plaques in the brain section as a result of the proteolytic cleavage of APP. A growing amount of evidence suggests that the APP processing and oligomerisation of A $\beta$  peptides induce fAD pathology, consequently leading to the formation of A $\beta$  plaques (Lashley *et al.*, 2018). Thus, understanding the pathology of A $\beta$  plaque formation and clearance is vital for elucidating the pathogenesis of AD.

Another pathological hallmark of AD is the formation of Neurofibrillary Tangles (NFTs) due to hyperphosphorylated tau. Tau is highly expressed in ocular neurons and the CNS (Muralidar *et al.*, 2020). It assists in stabilising the neuronal microtubules in dendrites and distal portions of axons (Pooler *et al.*, 2014). The abnormal folding, aggregation and oligomerisation of tau lead to the formation of hyperphosphorylated tau (Iqbal *et al.*, 2013; Wit & Ghosh, 2015). Subsequently, NFT is formed in AD patients due to the dysregulation of tau phosphorylation, characterised by the imbalance that favours excessive phosphorylation over dephosphorylation (Muralidar *et al.*, 2020).

Although both hallmarks hold a pivotal role in AD pathogenesis, AD research is more focused on investigating A $\beta$  pathogenesis due to the perceived earlier onset compared to the formation of NFTs. It is relevant to highlight that the accumulation of A $\beta$  plaques induces tau pathology in multiple APP transgenic animal models, but tau does not influence A $\beta$  pathology (Guo *et al.*, 2020). Hence, the dominant pathological formation of A $\beta$  plaques makes them and the APP processing pathway more compliant targets for therapeutic interventions aimed at alleviating AD development.

### 2.5.2 Amyloid Precursor Protein (APP)

The APP is instrumental in AD pathogenesis. This type-1 transmembrane glycoprotein contains an extracellular N-terminus that spans the membrane once (Zhao *et al.*, 2020). Located on chromosome 2 and encodes around 695–770 amino acids (Müller *et al.*, 2017; Tan & Azzam, 2017), the APP exhibits multifaceted roles in neuronal physiology, including transmembrane signal transduction, calcium metabolism, neuronal protein trafficking along the axon, cell adhesion, synaptogenesis, and neuronal growth, highlighting its significance that extends beyond amyloidogenesis (Zheng & Koo, 2006; Cho *et al.*, 2022).

At the gene level, the APP mRNA undergoes alternative splicing to produce various isoforms with distinct lengths and functions. For instance, the APP<sub>695</sub>, APP<sub>751</sub>, and APP<sub>770</sub> contain 695, 751, and 770 amino acids, respectively (Wang *et al.*, 2017). Whereas at the protein level, tightly regulated Post-translational Modifications (PTMs) determines the APP isoforms. For instance, N-glycosylation leads to immature APP (imAPP) formation and N- and O-linked glycosylation and phosphorylation leads to mature APP (mAPP) formation (Haass *et al.*, 2012; Gołacka *et al.*, 2021). The mAPP expressed at transmembrane undergoes proteolytic cleavage by  $\alpha$ - and  $\beta$ -secretase at the plasma membrane and  $\gamma$ -secretase at the late secretory pathway in the APP processing pathway (Khambhati *et al.*, 2023).

### 2.5.3 APP cleaving proteases

Several key enzymes are involved in APP metabolism, such as  $\alpha$ -secretase,  $\beta$ -secretase, and  $\gamma$ -secretase (Table 2.1). The  $\alpha$ -secretase is a type-I transmembrane protein and a zinc metalloproteinase that cleaves APP in the non-amyloidogenic pathway (Guo *et al.*, 2020). It is also grouped in the A Disintegrin and Metalloproteinase (ADAM) family, encompassing several members with  $\alpha$ -secretase-like activities, such as ADAM9, ADAM10, and ADAM17 (Zhang *et al.*, 2011). Studies have reported that the expression of ADAM10 is significantly reduced in the CSF of AD patients compared to healthy people (Hershkovits *et al.*, 2023), underscoring its inhibition in AD pathogenesis.

$\beta$ -secretase is a type-I transmembrane aspartyl protease linked to the membrane near the C-terminus domain. BACE1, an active gene that codes for the protease of  $\beta$ -secretase (Kamble *et al.*, 2024), proteolyzes APP at the N-terminus domain (Zhang *et al.*, 2019). The overexpression of BACE1 enhances the activity of  $\beta$ -secretase in the Golgi apparatus and endosomes, leading to over-proteolysis of APP. Although BACE2 is a homologue of BACE1 and is found in the critical region for Down's syndrome (Lashley *et al.*, 2018), it is not coded for  $\beta$ -secretase. Previous findings have suggested that inhibiting the BACE1 gene prevents the production of toxic A $\beta$  peptides, restores memory functions and APP processing, and enhances insulin sensitivity in BACE1 knock-in mice (Dekeryte *et al.*, 2021).

The  $\gamma$ -secretase is an aspartyl protease comprising four complex transmembrane subunits, including nicastrin, anterior pharynx-defective-1 (APH1), presenilin enhancer 2 (PEN2), and presenilin (PSEN) (Hur, 2022). Both PSEN1 and PSEN2 are homologues of PSEN subunits that cleave their substrates at the transmembrane region. Mutations in the

chromosomes of PSEN1 (14q24.3) and PSEN2 (1q31–q42) result in numerous irregularities and dysfunctions, which lead to AD pathogenesis. PSEN1 mutation alone constitutes over 80% of all reported mutations in fAD. Among all the reported PSEN1 mutations, the A246E mutation gained pivotal focus which was first identified in 1995 (Sherrington *et al.*, 1995). The gain-of-toxic-function hypothesis suggests that mutations in fAD primarily enhance the production of aggregation-prone A $\beta$  peptides and toxic oligomers implicated in AD (Selkoe & Hardy, 2016; Dehury *et al.*, 2020). Thus, therapeutic strategies targeting the inhibition of PSEN catalytic subunits should be highly specific (Hur, 2022).

Table 2.1 List of cleavage enzymes, isoforms, functions and its relevant information

<b>Cleavage enzymes</b>	<b>Isoforms</b>	<b>Functions</b>	<b>Relevant information</b>	<b>References</b>
$\alpha$ - secretase	ADAM9	Controlled proteolysis without producing sAPP $\alpha$	Endoprotease bound to plasma membrane	Guo <i>et al.</i> , 2020
	ADAM10	Cleaves APP at A $\beta$ domain (Lysine 16 and Leucine 17), produces sAPP $\alpha$ & CTF $\alpha$	Most active $\alpha$ -secretase isoform, precursor (~100 kDa), processed (~80 kDa), and active (~60 kDa)	Zhang <i>et al.</i> , 2011; HersHKovits <i>et al.</i> , 2023; Peron <i>et al.</i> , 2018
	ADAM17	Key regulator of APP proteolysis	Dysregulation affects APP metabolism	Endres & Deller, 2017
$\beta$ - secretase	BACE1	Cleaves APP at Methionine 596 and Aspartic acid 597, produces sAPP $\beta$ & CTF $\beta$	Rate-limiting enzyme in APP metabolism, overexpression elevates $\beta$ -secretase activity	Guo <i>et al.</i> , 2020; Zhang <i>et al.</i> , 2019; Kamble <i>et al.</i> , 2024
	BACE2	Cleaves APP at $\theta$ -site (Phenylalanine 20) and prevents A $\beta$ production	Less intense activity in AD pathogenesis	Lashley <i>et al.</i> , 2018; Wang <i>et al.</i> , 2019
$\gamma$ - secretase	PSEN1	Cleaves APP at transmembrane domains at positions 6 and 7	Mutations in PSEN1 (14q24.3) elevate A $\beta$ 42 and A $\beta$ 40	Lin <i>et al.</i> , 2021; Hur, 2022

<b>Cleavage enzymes</b>	<b>Isoforms</b>	<b>Functions</b>	<b>Relevant information</b>	<b>References</b>
$\gamma$ - secretase	PSEN2	Cleaves APP at transmembrane domains	Mutations in PSEN2 (1q31–q42) cause AD	Sushma & Mondal, 2019; Zhou <i>et al.</i> , 2020; AlzForum, 2023
	Nicastrin	Active receptor interacting with APP sequestrates	Required for $\gamma$ -secretase activity	Aßfalg <i>et al.</i> , 2024
	APH1	Aids nicastrin localisation	Supports $\gamma$ -secretase complex	Hur, 2022
	PEN2	Matures nicastrin, enables PSEN expression	Integral in $\gamma$ -secretase function	Aßfalg <i>et al.</i> , 2024

#### 2.5.4 APP processing pathways

The APP metabolism takes place primarily via two proteolytic processing pathways: non-amyloidogenic and amyloidogenic (Figure 2.1) (Müller *et al.*, 2017). The APP is predominantly cleaved by  $\alpha$ -secretase in the non-amyloidogenic pathway, producing a shorter C-terminal fragment- $\alpha$  (CTF $\alpha$ ) and a longer soluble APP-  $\alpha$  (sAPP $\alpha$ ). Then, the  $\gamma$ -secretase complex further cleaves the CTF $\alpha$  to form an APP Intracellular Domain (AICD) and p3 peptide (Cho *et al.*, 2022). The sAPP $\alpha$  and CTF $\alpha$  fragments were reported to enhance synaptic plasticity, maintain neuronal excitability, and protect neurons against metabolic and oxidative injuries, memory, and learning (Folch *et al.*, 2018; Ribarič, 2018). The sAPP $\alpha$  inhibits BACE1 in the amyloidogenic pathway, reduces the formation induced by sAPP $\beta$  peptides, and restores the balance to the APP processing in pre-injury response for hypoxia (Libeu *et al.*, 2015).

In the amyloidogenic pathway, the APP is cleaved by  $\beta$ -secretase at the N-terminal of the A $\beta$  domain, generating a C-terminal fragment- $\beta$  (CTF $\beta$ ) and soluble APP- $\beta$  (sAPP $\beta$ ) as the by-products (Lashley *et al.*, 2018; Cho *et al.*, 2022). The CTF $\beta$  fragments are further proteolyzed by  $\gamma$ -secretase to form varying lengths of A $\beta$  peptides and AICD (Zhao *et al.*, 2020). As the APP accumulates, toxic A $\beta$  peptides are produced in acidic neuronal compartments, such as lysosomes and late endosomes (Poulsen *et al.*, 2017). The mechanism of APP expression in AD pathogenesis remains obscure. Simultaneously, an increase in the production of toxic sAPP $\beta$ -induced stress levels in the ER (Botteri *et al.*, 2019). The overproduction of CTF $\beta$  also caused abnormalities in the endosomal A $\beta$  production (Jiang *et al.*, 2019; Kwart *et al.*, 2019) and impaired neuronal functions (Takauji *et al.*, 2023).

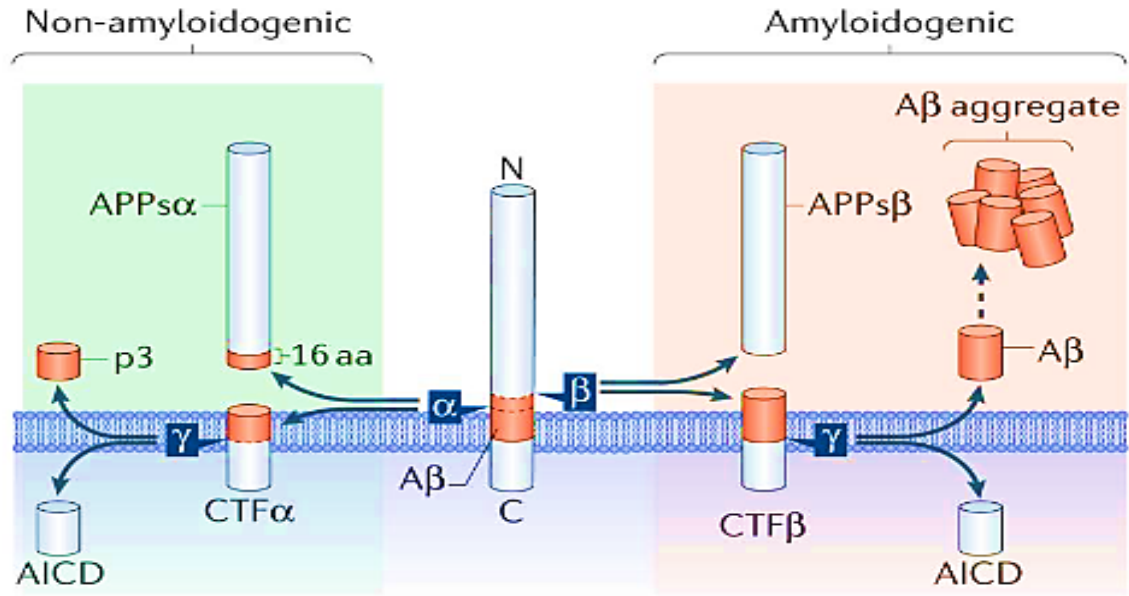


Figure 2.1 Schematic diagram of the APP processing pathway comprising the amyloidogenic pathway (pink background) and non-amyloidogenic pathway (green background). Adapted from Müller *et al.* (2017).

## 2.6 Amyloid-beta (A $\beta$ )

### 2.6.1 Amyloid cascade hypothesis

A $\beta$  peptides are one of the significant hallmarks of AD. Hardy & Higgins (1992) proposed the amyloid cascade hypothesis, which links the accumulation of A $\beta$  peptides in the brain parenchyma to the primary event in AD pathogenesis. This hypothesis emphasises the critical imbalance between the production and clearance of A $\beta$  peptides, ultimately leading to the complex neuropathology observed in AD. Despite over three decades of relentless studies on AD, researchers are unable to provide a convincing explanation of the etiopathogenic events involving the formation and advancement of disease apart from A $\beta$  plaque aggregation.

### 2.6.2 A $\beta$ conformations

The A $\beta$  peptide comprises 37–49 amino acid residues and is formed through the proteolysis of APP by  $\beta$ -secretase and  $\gamma$ -secretase in the amyloidogenic pathway. The A $\beta$ 40 is the primary A $\beta$  isoform, which is made up of 40 amino acids. However, the altered proteolysis of APP generates a minor isoform called A $\beta$ 42, which comprises 42 amino acids (Chen *et al.*, 2017). The two-residue variation between A $\beta$ 40 and A $\beta$ 42 leads to enormous differences in their clinical and biological actions.

Figure 2.2 shows the structural confirmation of A $\beta$  peptides. It first exists in the form of monomers, which then accumulate to form oligomers in both normal and AD brains (Chen *et al.*, 2017). The A $\beta$  fibrils are insoluble and large and tend to aggregate to form amyloid plaques. In contrast, A $\beta$  oligomers are soluble, hydrophobic peptides and may rapidly diffuse through the cell membrane and the brain region. They can also rapidly aggregate into protofibrils and fibrils to form amyloid plaques. Thus, A $\beta$  oligomers represent the most toxic confirmation of A $\beta$  peptides (Bode *et al.*, 2017). Meanwhile, unbranched, long fibrils break down the myelin sheath of neurons, damage synaptic terminals, and cause neurodegeneration. Following the APP proteolysis, the newly produced A $\beta$  peptides are secreted into the extracellular space or bound to the plasma membrane or other extracellular components, such as cellular membranes, receptors, and metal ions that offer binding sites for soluble A $\beta$  (Chen *et al.*, 2017).

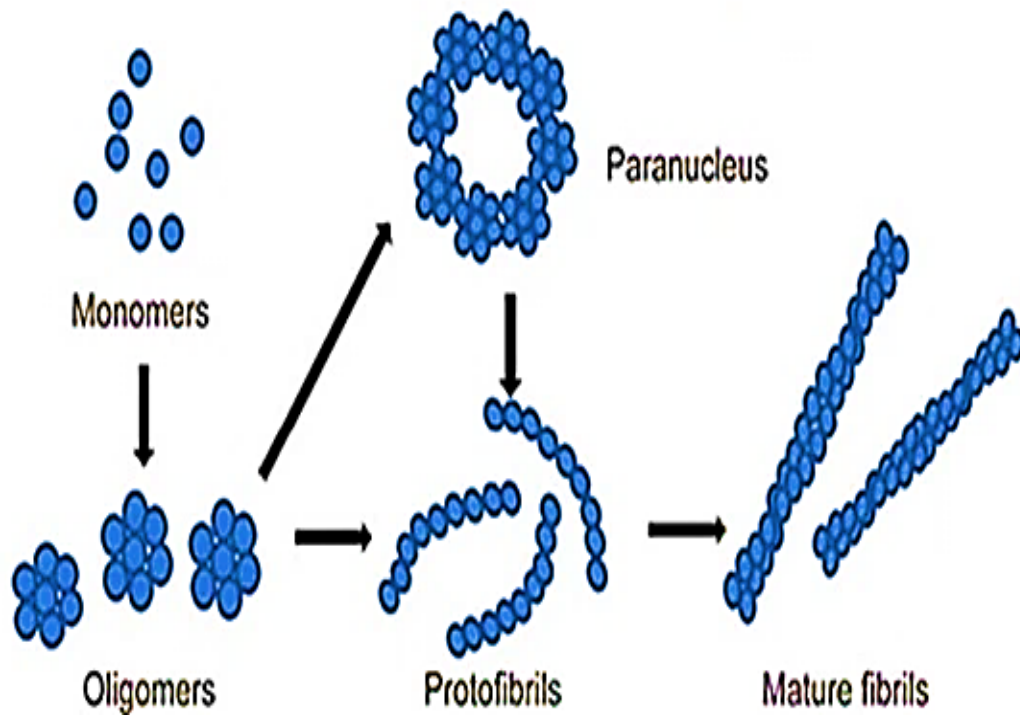


Figure 2.2 The structural confirmation of A $\beta$  peptides. Adapted from Chen *et al.* (2017).

### 2.6.3 A $\beta$ toxicity

The A $\beta$  peptides are highly unstable, self-aggregating molecules that cause toxicity by dissociating into various isoforms. Lambert *et al.* (1998) published the first report on A $\beta$  toxicity, which showed potent neurotoxin effects on the CNS. The oligomerisation of A $\beta$  occurs mainly at the plasma membrane (Bode *et al.*, 2017), producing a wide range of A $\beta$  oligomeric isoforms with different neurotoxicity levels and aggregation behaviours. The hydrophobic nature of A $\beta$  oligomers makes them highly diffusible, leading to higher interactions at the phospholipid bilayer membrane of the cells and induce neuroinflammation (Salahuddin *et al.*, 2016; Yang *et al.*, 2017).

Decades of ongoing studies have revealed the harmful impacts of various A $\beta$  isoforms, specifically A $\beta$ 40 and A $\beta$ 42, on the human brain (Matuszyk *et al.*, 2022). In particular, the A $\beta$ 40 can induce nuclear damage to the DNA in oligodendrocytes, which drastically reduces cell survival (Xu *et al.*, 2019). On the other hand, A $\beta$ 42 initiates the *in vivo* cascade of neuronal death in the brain's hippocampal region and loss of neuronal viability *in vitro* (Brouillette *et al.*, 2012; Matuszyk *et al.*, 2022). Numerous evidence also suggest that A $\beta$ 42 have a greater impact on synaptic losses and is the most cytotoxic compared to its A $\beta$ 40 counterpart (Yang *et al.*, 2017; Bate & Williams, 2018). This advantage prompted the preferential use of A $\beta$ 42 in neurotoxicity studies of potential AD therapeutics. Acknowledging the limited understanding of A $\beta$ , more future studies are needed to address the potential knowledge gaps in AD.

## 2.7 Oxidative Stress (OS)

Reactive Oxidative Stress (ROS) are highly active oxygen metabolites in terms of oxidative modifications of cellular macromolecules (Cheignon *et al.*, 2018). However, when the biological defences of the cell are overwhelmed by pro-oxidants, such as ROS, this leads to Oxidative Stress (OS) (Singh *et al.*, 2019). The OS hypothesis in AD suggests that mitochondria produce more ROS as they are damaged over time (Otín *et al.*, 2013). The high accumulation of neurotoxic A $\beta$  peptides forms A $\beta$  ion channels on the membrane, leads to a greater Ca<sup>2+</sup> influx into mitochondria (Salahuddin *et al.*, 2016). Hence, the disrupted Ca<sup>2+</sup> homeostasis and formation of A $\beta$  ion channels compromise the physiological function of the organelles in neurons and peripheral cells.

OS in fAD is also attributed to the presence of mutations in APP, PSEN1, and PSEN2. These mutations were found to significantly elevate mitochondrial ROS production and trigger antioxidant enzyme dysfunction in triple transgenic mice carrying APP, PSEN1, and MAPT mutations (Han *et al.*, 2021). A positive feedback loop exists between A $\beta$  and OS, where elevated levels of A $\beta$ 40 and A $\beta$ 42 led to an increase in OS in CNS and peripheral cells (Perluigi *et al.*, 2024). The increased accumulation of A $\beta$  peptides induces lipid peroxidation on the neuronal and peripheral cell membranes. This process triggers higher OS, which results in membrane permeabilisation, leading to the formation of transmembrane pores. Thus, effective strategies must be implemented to prevent or reduce OS damage and provide therapeutic efficacy against AD. In this context, the viable strategy to overcome OS-caused abnormalities can be considered, including downregulating A $\beta$  production, enhancing the antioxidant system, and improving mitochondria functionality.